Electrocatalytic Features of a Heme Protein Attached to Polymer–Functionalized Magnetic Nanoparticles

ARTICLE *in* ANALYTICAL CHEMISTRY · NOVEMBER 2013

Impact Factor: 5.64 · DOI: 10.1021/ac402421z · Source: PubMed

2 AUTHORS:

Sadagopan Krishnan
Oklahoma State University - Stillwater
66 PUBLICATIONS **502** CITATIONS
SEE PROFILE

Charuksha Walgama
Oklahoma State University - Stillwater
25 PUBLICATIONS **16** CITATIONS
SEE PROFILE

analytical chemistry

Article

pubs.acs.org/ac

Electrocatalytic Features of a Heme Protein Attached to Polymer-Functionalized Magnetic Nanoparticles

Sadagopan Krishnan* and Charuksha Walgama

Department of Chemistry, Oklahoma State University, Stillwater, Oklahoma 74078, United States

ABSTRACT: Direct electron-transfer and electrocatalytic kinetics of covalently attached myoglobin (MB) films on magnetic nanoparticles (MB-MNP$_{covalent}$), in comparison to the corresponding physisorbed films and individual components, are reported for the first time. MB-MNP$_{covalent}$ ("-" denotes a covalent linkage) was adsorbed onto a cationic poly(ethyleneimine) layer (PEI) coated high-purity graphite (HPG) electrode. Similarly, films of myoglobin physisorbed on magnetic nanoparticles (MB/MNP$_{adsorbed}$, "/" denotes a noncovalent nature), only MB, or only MNP were constructed on HPG/PEI electrodes for comparison. The observed electron-transfer rate constants (k_s, s^{-1}) were in the following order: MB-MNP$_{covalent}$ (69 ± 6 s^{-1}), MB/MNP$_{adsorbed}$ (37 ± 2 s^{-1}), only MB (27 ± 2 s^{-1}), and only MNP (16 ± 3 s^{-1}). The electrocatalytic properties of these films were investigated with the aid of *tert*-butylhydroperoxide as a model reactant, and its reduction kinetics were examined. We observed the following order of catalytic current density: MB-MNP$_{covalent}$ > MB/MNP$_{adsorbed}$ > only MNP > only MB, in agreement with the electron-transfer (ET) rates of MB-MNP$_{covalent}$ and MB/MNP$_{adsorbed}$ films. The crucial function of MNP in favorably altering the direct ET and electrocatalytic properties of both covalently bound MB and physisorbed MB molecules are discussed. In addition, the occurrence of a highly enhanced electron-hopping mechanism in the designed covalent MB-MNP$_{covalent}$ films over the corresponding physisorbed MB/MNP$_{adsorbed}$ film is proposed. The enhanced electron-transfer rates and catalytic current density suggest the advantages of using metalloenzymes covalently attached to polymer-functionalized magnetic nanoparticles for the development of modern highly efficient miniature biosensors and bioreactors.

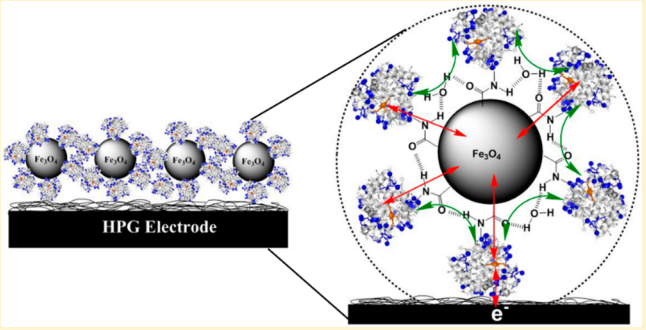

Obtaining mechanistic insights on the electron-transfer and catalytic properties of redox enzyme films on electrodes can aid in the understanding of complex *in vivo* redox processes as well as in the design of useful biosensors and bioreactors.[1−3] Under these aspects, the direct electrochemistry of redox enzyme films on electrodes has been extensively studied. Moreover, developing efficient enzyme based, clean bioreactors for the green syntheses of drug metabolites and precious fine chemicals with high stereospecificity possess an enormous potential to change the present paradigm of the pharmaceutical field and boost the country's economy. To develop efficient electrochemical bioreactors with high catalytic efficiency in a minimal reactor volume, elegant tailoring of remarkable enzyme catalysts with nanomaterials is highly promising. In particular, the role of magnetic particles (nano- and microparticles) in the development of modern ultrasensitive electrochemical and optical biosensors is immense, and more research avenues both on the fundamental and applied aspects remain to be explored.[4−9]

Heme proteins conjugated to magnetic nanoparticles (MNP) have been useful in the development of highly sensitive point-of-care biosensors[10] and for the efficient stereoselective synthesis of drug metabolites and chemical compounds.[11] Additionally, the intrinsic peroxidase-like activity of MNP enables the application in diagnostic tools and other biomedical applications.[12−14] Among several heme proteins, myoglobin (MB) has been a good electrochemical model protein due to its easy commercial availability, peroxidase-like catalytic activity, and established X-ray crystal structures.

Magnetic microsphere-antibody conjugates have been utilized for fluorescence based detection of MB and heart-type fatty acid-binding proteins relevant to acute myocardial infarction.[15] An MNP-based fluoroimmunoassay for detecting serum MB has also been reported.[16] In addition, the binding properties of MB with MNP have demonstrated utility as magnetic resonance imaging markers to visualize mice heart and myocardium.[17]

Glassy carbon electrodes coated with the magnetic core−shell Fe_3O_4@Al_2O_3 or Fe_3O_4@Au nanoparticles were used to examine the direct electrochemistry of immobilized hemoglobin (Hb), horseradish peroxidase (HRP), and MB.[18,19] The same group later reported the application of bifunctional Fe_3O_4@ZrO_2 nanoparticles[20] and multifunctional heme protein-Au-polydopamine-Fe_3O_4 magnetic nanoparticles[21] to evaluate the direct electrochemistry of heme proteins including MB. Similarly, glassy carbon electrodes coated with poly-

Received: August 1, 2013
Accepted: November 9, 2013
Published: November 10, 2013

   dx.doi.org/10.1021/ac402421z | *Anal. Chem.* 2013, 85, 11420−11426

Scheme 1. MB and MNP Films Constructed on the Polymer (PEI)-coated HPG Electrodes for Direct Electrochemical Investigation: (A) MB-MNP$_{covalent}$, (B) MB/MNP$_{adsorbed}$, (C) only MB, and (D) only MNP

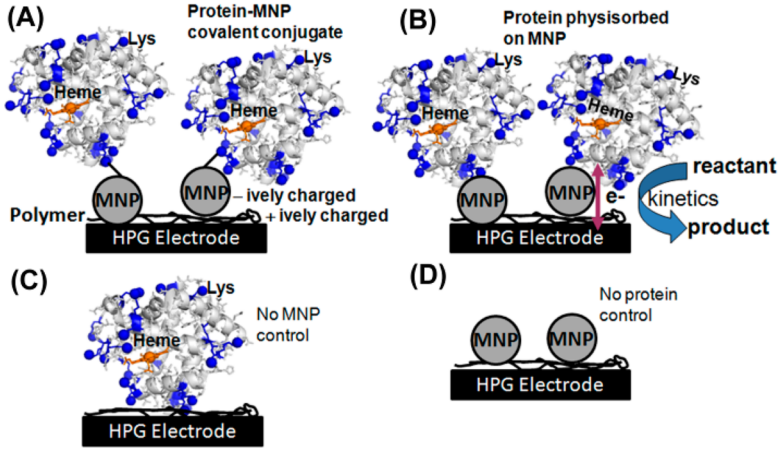

(dimethyldiallylammonium chloride) and Fe_3O_4@SiO_2 magnetic nanoparticles were employed to adsorb MB in solution. These electrodes were reported to be useful for peroxide detection with high thermostability.[22]

Although prior reports addressed many useful sensing and direct electrochemistry aspects of MNP on heme proteins, we report here the first mechanistic insights with respect to the covalent attachment and physisorption of MB onto MNP and their comparative electrochemistry with films of either MB or MNP alone on electrodes. In this paper, the enhanced electron-transfer and catalytic rates for MB films covalently attached to poly(acrylic acid)-functionalized MNP and coated on HPG/PEI electrodes are presented. To gain insight, systematic comparisons were made with MB films physisorbed on poly(acrylic acid)-functionalized MNP, only MB film, or only MNP film coated on similar electrodes. Scheme 1 illustrates the four types of films that were constructed on HPG/PEI electrodes and investigated in this study for the first time.

EXPERIMENTAL SECTION

Chemicals and Materials. Polyacrylic acid-functionalized magnetic nanoparticles (MNP, 100-nm hydrodynamic diameter) were purchased from Chemicell GmbH Inc. (Berlin, Germany). Equine heart myoglobin (MB), *tert*-butylhydroperoxide (t-BuOOH), poly(ethyleneimine) (PEI), 1-ethyl-3-[3-dimethylaminopropyl] carbodiimide hydrochloride (EDC), and *N*-hydroxysuccinimide (NHS) were purchased from Sigma. High-purity graphite disk electrodes (HPG, geometric area 0.2 cm^2) were purchased from McMaster-Carr (Atlanta, GA). All other chemicals were of analytical grade.

To obtain steady-state reduction currents for various oxygen concentrations, known percent mixtures of oxygen in nitrogen were supplied to the electrochemical cell using two mass flow controllers (Aalborg Instruments and Controls Inc., NY). The percent oxygen was converted into concentration using Henry's law.[23,24] Unless otherwise specified, all electrochemical measurements were performed with an anaerobic phosphate buffer saline (PBS) electrolyte, pH 7.4 at 25 °C, under a N_2 atmosphere. The current density data presented in this work are with respect to the geometric area of electrodes (0.2 cm^2).

Instrumentation. A CH instrument 6017 electrochemical analyzer was used to perform cyclic voltammetry (CV) studies. To conduct peroxide reduction kinetics catalyzed by MB films, rotating-disk electrochemistry (RDE) was used. The RDE experiments were performed with an Autolab rotor attached to a rotation controller unit. A sealed electrochemical cell employing a Ag/AgCl reference electrode (1 M KCl, CH Instruments Inc.), a Pt-wire counter electrode, and a MB film-coated HPG working electrode was used. PBS solutions were purged with high-purity nitrogen for 30 min before the voltammograms were acquired, and a continuous nitrogen atmosphere was maintained during measurements.

Covalent Attachment of Myoglobin to Magnetic Nanoparticles (MB-MNP$_{covalent}$). The surface lysine residues of MB (PDB 2FRF)[25] were covalently attached to the carboxylic acid groups of polyacrylic-acid functionalized MNP according to the manufacturer's protocol (Chemicell GmbH Inc.) (Scheme 1A). Briefly, a freshly prepared aqueous solution (300 μL) containing EDC (0.35 M) and NHS (0.1 M) was added to 2 mg of MNP and incubated for 15 min to activate the carboxylic acid groups of MNP by converting them into N-succinimidyl esters, which are facile leaving groups. The activated nanoparticles were separated from the unreacted EDC/NHS solution by application of a magnetic field. Then the particles were washed in water and immediately suspended in MB solution (1 mL of 3 mg mL^{-1} in pH 5.0 acetate buffer). The covalent attachment of MB to MNP was conducted for 2 h at room temperature with continuous gentle mixing. The MB-attached particles were separated from the free MB in solution by employing a magnetic field provided by a magnet.

The MB-MNP$_{covalent}$ conjugate was washed twice in PBS, resuspended in a fresh PBS solution (200 μL), and then used for electrochemical studies. Similarly MB films physisorbed on MNP (no EDC/NHS step) (denoted as MB/MNP$_{adsorbed}$) were prepared under similar conditions. A pH 5.0 condition was used to make MB solutions in order to obtain a net positive charge of MB (isoelectric points, pI = 6.8 and 7.2),[26,27] and thus facilitate its interaction with the negatively charged poly(acrylic acid) groups (pK_a 4.3)[28] of MNP during the covalent attachment or the physisorption process. Once the MB-MNP$_{covalent}$ conjugate and MB/MNP$_{adsorbed}$ systems were prepared, they were resuspended in physiological pH 7.4 (PBS) to obtain a net negative surface charge of MB-MNP$_{covalent}$ and MB/MNP$_{adsorbed}$ films suitable to immobilize onto positively charged PEI (a cationic polymer) coated HPG electrodes. For comparison, free MB solution and free MNP suspension in PBS were prepared under similar conditions and used for electrochemical measurements.

dx.doi.org/10.1021/ac402421z | Anal. Chem. 2013, 85, 11420−11426

Preparation of MB Films on HPG Electrodes (Scheme 1). Prior to use, HPG electrodes were freshly polished on a P320 grit SiC paper, ultrasonicated for 30 s in ethanol, followed by 30 s in water, and then the electrodes were dried under nitrogen. A solution of PEI (2 mg mL^{-1} in water) was placed on the polished electrode and allowed to electrostatically adsorb for 15 min. To the PEI-adsorbed HPG electrodes (HPG/PEI), a 15-μL suspension of MB-$MNP_{covalent}$ conjugate in PBS was added and allowed to immobilize for 30 min. The electrodes were rinsed with water between each adsorption step to remove weakly and unbound molecules. Similarly, the PEI-coated HPG electrodes were used to immobilize films of MB/$MNP_{adsorbed}$ or only MB or only MNP.

RESULTS

Quantitation of MB Bound to MNP. The amounts of bound MB in MB-$MNP_{covalent}$ and MB/$MNP_{adsorbed}$ films were estimated by use of a UV−vis spectrophotometer (Thermo Scientific, model Evolution 60S). From the difference in Soret band-absorbance of free MB in solution at 410 nm before and after coating to MNP, it was determined that 23 ± 3 nmol of MB were covalently attached to MNP in MB-$MNP_{covalent}$ films and 13 ± 2 nmol of MB were physisorbed with MNP in MB/$MNP_{adsorbed}$ films. This quantitation suggests that covalent attachment enables the high-density loading of protein molecules onto MNP as opposed to physisorption. This can be attributed to the large number of available activated −COOH groups on MNP and less sites of contact required between MB and MNP in the covalent mode of linking (only the surface Lys residues of MB are involved in the amide-bond formation with activated −COOH groups of MNP).

On the other hand, the physisorption of MB with MNP may involve contacts between multiple surface amino acid groups of MB with the surface of MNP to form an electrostatic network. This could induce a sterically restricted arrangement of MB molecules on the MNP surface and hence the detected less amount of bound MB molecules. Using the data provided by the manufacturer (Chemicell Inc.) on the number of MNP present per g weight (~1.8×10^{15}) and by assuming a uniform distribution of MB molecules on MNP, we calculated that ~3860 MB molecules could be bound per MNP in MB-$MNP_{covalent}$ conjugate and ~2350 MB molecules could be bound per MNP in the MB/$MNP_{adsorbed}$ system.

Electrochemical Properties. Figure 1 represents the background subtracted cyclic voltammograms (CVs) of MB-$MNP_{covalent}$, MB/$MNP_{adsorbed}$, only MB, or only MNP films coated on HPG/PEI electrodes. Nearly the same midpoint potential ($E^{\circ\prime}$) of −0.34 V (±0.01) versus Ag/AgCl in PBS was observed for all MB films (MB-$MNP_{covalent}$, MB/$MNP_{adsorbed}$, and only MB) (N = 3 repeats). On the other hand, a more positive $E^{\circ\prime}$ of −0.27 V (±0.01) versus Ag/AgCl was observed for the MNP film alone (N = 3 repeats). The Fe_3O_4 MNP used in this study consisted of two iron atoms in the 3+ state and one iron atom in the 2+ state[29] and hence were identified to exhibit reversible voltammetry, however, at a more positive $E^{\circ\prime}$ than MB films. The observed characteristic $E^{\circ\prime}$ suggests that the voltammetric features correspond to MB in MB-$MNP_{covalent}$ and MB/$MNP_{adsorbed}$ films (Figure 1).

For all the MB and MNP films examined, the peak current versus scan rate was linear in the scan rate range of 0.02 to 2 V s^{-1} and the oxidation to reduction peak-current ratio was near 1. Reduction peak potentials shifted more negative with increasing scan rate, and peak widths at half-maximum were

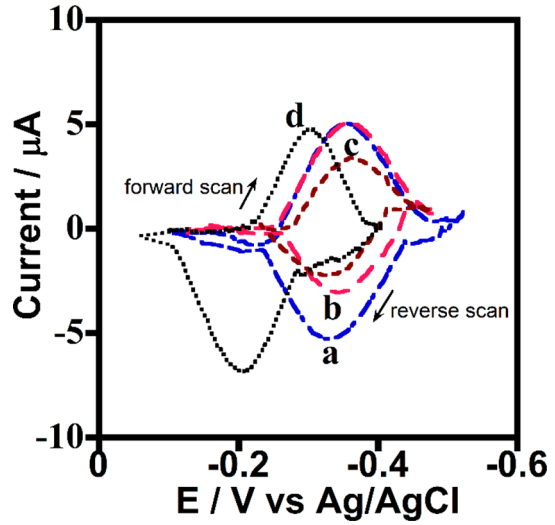

Figure 1. Background-subtracted thin-film cyclic voltammograms of (a) MB-$MNP_{covalent}$, (b) MB/$MNP_{adsorbed}$, (c) only MB, and (d) only MNP films immobilized on PEI-coated HPG electrodes in anaerobic PBS at 25 °C; scan rate, 0.3 V s^{-1}.

in the range of 100−120 mV (slightly greater than the ideal one-electron value of 90.6/n mV).[30] These electrochemical properties correspond to the nonideal quasi-reversible thin-film surface voltammetry of MB-$MNP_{covalent}$, MB/$MNP_{adsorbed}$, only MB, or only MNP films on HPG/PEI electrodes.[31−34]

The average electroactive amounts (±5−8% SD) of MB in different films were determined to be in the following order: MB-$MNP_{covalent}$ (129 pmol cm^{-2}) > MB/$MNP_{adsorbed}$ (78 pmol cm^{-2}) > MB film alone (36 pmol cm^{-2}). The electroactive amount of MNP film alone was 57 pmol cm^{-2}. The higher electroactive amount of MB-$MNP_{covalent}$ film over the MB/$MNP_{adsorbed}$ film additionally suggested a greater proportion of connected heme centers of MB-$MNP_{covalent}$ film with the electrode surface. About 3.6-times enhancement in the electroactive amount of MB was observed as a result of covalent attachment to MNP over the free MB film on HPG/PEI electrodes. This property suggested that MNP in MB-$MNP_{covalent}$ film carried a large excess of covalently attached MB to get immobilized on HPG/PEI electrodes to give high electroactive protein amount. The physisorbed films of MB in the MB/$MNP_{adsorbed}$ system showed a smaller enhancement in electroactive amount (by 2.2-times) over the free MB film.

Moreover, to obtain clearly measurable peak-potentials for direct ET rate calculation from the CVs of free MB films on HPG/PEI electrodes (Figure 1), it was deemed necessary to use a 7 times greater amount of MB in PBS solution (161 nmol in 200 μL of PBS) in comparison to the amount of MB (23 nmol) immobilized on MB-$MNP_{covalent}$ films. This property suggests the general advantage of using relatively inexpensive MNP to conjugate a minimal amount of expensive metalloenzyme catalysts to obtain superior direct electrochemical activity. It was found that for comparative catalytic O_2 and peroxide reduction kinetics of free MB in solution (detail below), 23 nmol of free MB (in 200 μL of PBS) provided measurable limiting currents, similar to the amount of bound MB in MB-$MNP_{covalent}$ films.

Rate of Direct Electron Transfer. The rate at which an electron transfer (ET) occurs between a protein film and an electrode (during oxidation and reduction) can be determined from the peak separation (ΔE_p) between the measured

dx.doi.org/10.1021/ac402421z | Anal. Chem. 2013, 85, 11420−11426

reduction ($E_{p,red}$) and oxidation ($E_{p,ox}$) values with increasing scan rate (i.e., potential ramp applied in V s^{-1}).[35] This rate calculation for surface-bound molecules was derived by Laviron based on the Butler–Volmer surface voltammetry, which assumes that a redox system can be characterized by a single ET rate constant that is the rate at the formal potential.[36]

A simplified relationship between the ET rate constant (k_s, s^{-1}) and peak separation for a surface-bound redox molecule on an electrode can be given as[36]

$$k_s = (nFm \times \text{scan rate})/RT \quad (1)$$

where n is the number of electrons involved in the ET, F is Faraday's constant (96 485 C mol^{-1}), R is the gas constant (8.314 J mol^{-1} K^{-1}), T is temperature in Kelvin, and m is a variable that is inversely related to the experimental peak separation (i.e., $m \propto 1/n\Delta E_p$) in a nonlinear fashion, as derived by Laviron.[36]

Thus, for a reversible redox process (fast reduction and oxidation), the peak separation between $E_{p,red}$ and $E_{p,ox}$ is small, m becomes large, and thus k_s is high. On the other hand, for a quasi-reversible or slow redox process of a protein film on an electrode, the peak separation increases with increasing scan rate and k_s is moderate to low.[31−35] Figure 2 shows the

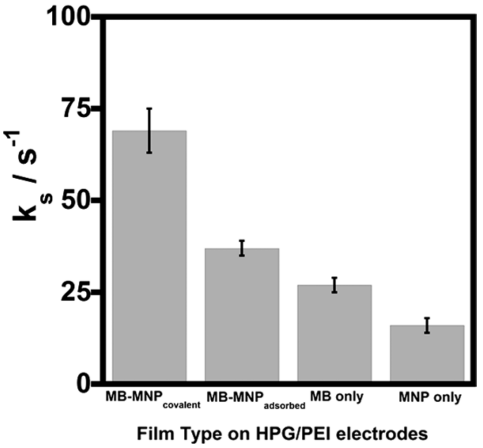

Figure 2. Direct electron-transfer rate constants (k_s) of MB-$MNP_{covalent}$, MB/$MNP_{adsorbed}$, only MB, or only MNP films on PEI-coated HPG electrodes in anaerobic PBS, 25 °C [avg ± SD for N = 3 repeats].

determined electron-transfer (ET) rate constants for MB-$MNP_{covalent}$, MB/$MNP_{adsorbed}$, only MB, or only MNP films on HPG/PEI electrodes. The k_s of each film was calculated from the peak separation in CVs with increasing scan rate after subtraction of a small nonkinetic constant peak separation obtained at slow scan rates, similar to that reported.[31−34]

Catalytic Oxygen Reduction. Oxygen reduction is a characteristic feature of heme proteins. The reduced Fe^{II}-heme protein can bind to oxygen to form an $Fe^{II}-O_2$ complex, which is electrochemically reduced on the electrode to regenerate Fe^{III}. This generates a catalytic current in proportion to the supplied oxygen concentration.[34] Figure 3 displays the oxygen concentration dependent, steady-state reduction currents catalyzed by the designed MB films. The following order of oxygen reduction current density was obtained: MB-$MNP_{covalent}$ > MB/$MNP_{adsorbed}$ > only MB > only MNP films. The MB-$MNP_{covalent}$ films exhibited the largest limiting oxygen-reduction currents in comparison to other MB films. This finding is in

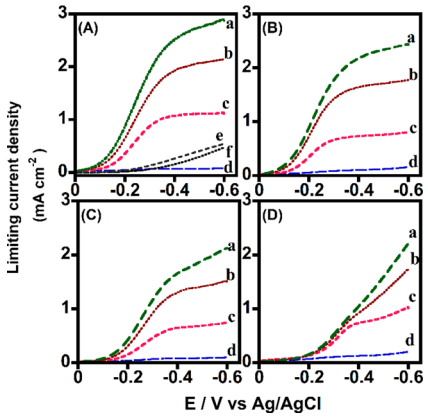

Figure 3. Rotating-disk catalytic oxygen-reduction voltammograms of (A) MB-$MNP_{covalent}$, (B) MB/$MNP_{adsorbed}$, (C) only MB, and (D) only MNP films with increasing oxygen concentration, (a) 900, (b) 600, (c) 300, and (d) 0 μM in PBS at 25 °C, 1000 rpm rotation rate, scan rate 0.1 V s^{-1}. Voltammograms e and f in part A correspond to voltammograms in 300 μM oxygen for (e) only HPG and (f) HPG/PEI, which did not exhibit any catalytic currents in the absence of MB and/or MNP in the film.

accordance with the extent of electroactively connected MB molecules in each film as detailed above.

Catalytic Peroxide-Reduction Kinetics. Catalytic peroxide-reduction rates of designed MB and MNP films on HPG/PEI electrodes were tested with t-BuOOH as a model reactant. Heme protein films, such as MB on electrodes, can catalytically reduce t-BuOOH to form *tert*-butanol.[31,37] This catalytic reduction can be monitored as an increase in limiting current in the RDE due to the formation and subsequent electrochemical reduction of reactive $^{\bullet}$MB-Fe^{IV}=O into MB-Fe^{III} in the presence of a peroxide.[31,38] Investigating the kinetics of t-BuOOH reduction to *tert*-butanol by heme protein films is straightforward and not complicated by the formation of several radical intermediates as in hydrogen peroxide reduction and discussed elsewhere.[32,37] Figure 4 displays representative rotating disk voltammograms for MB and MNP films with increasing t-BuOOH concentration.

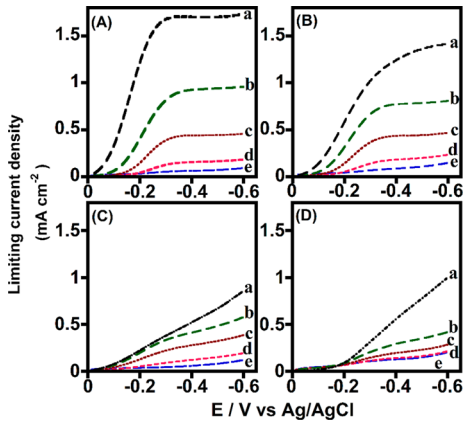

Figure 4. Representative steady-state catalytic reduction voltammograms for (A) MB-$MNP_{covalent}$, (B) MB/$MNP_{adsorbed}$, (C) only MB, and (D) only MNP films immobilized on PEI-coated HPG electrodes with increasing t-BuOOH concentration in oxygen free PBS, 25 °C, scan rate 0.1 V s^{-1}, 1000 rpm rotation rate: (a) 2.8, (b) 1.0, (c) 0.4, (d) 0.1, and (e) 0 mM.

dx.doi.org/10.1021/ac402421z | Anal. Chem. 2013, 85, 11420−11426

We observed that the increase in limiting reduction current with increasing concentration of t-BuOOH followed Michaelis–Menten kinetics (Figure 5). Electrochemical Michaelis–Menten kinetics relating the catalytic current (I_{cat}) to reaction rate parameters is given by[37,39,40]

$$I_{cat} = \frac{nFA\Gamma(k_{cat}/K_M)C_s}{(1/K_M)C_s + 1} \quad (2)$$

where n is the number of electrons transferred in a catalytic reaction (n = 2 for peroxide reduction by heme proteins), F is Faraday's constant, A is electrode area (0.2 cm^2), Γ is the electroactive enzyme amount coated on an electrode (in nmol cm^{-2}), C_s is the reactant concentration in solution (in mM), k_{cat} is the catalytic rate constant (s^{-1}), and K_M is the Michaelis–Menten constant. The Γ is obtained from the peak area (Q, corresponding to the charge in coulombs) for reduction in the cyclic voltammogram of a redox protein and using the equation, $Q = nFA\Gamma$.[31]

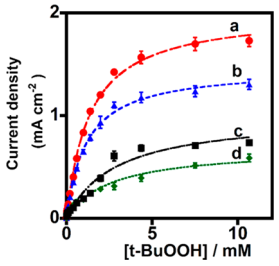

Figure 5. Michaelis–Menten electrochemical kinetics for peroxide reduction by (a) MB-$MNP_{covalent}$, (b) MB/$MNP_{adsorbed}$, (c) only MNP, and (d) only MB films for the data shown in Figure 4 (avg ± SD for N = 3 repeats).

DISCUSSION

Enhanced ET Rates and Electron-Hopping. Myoglobin covalently attached to magnetic nanoparticles in MB-$MNP_{covalent}$ films and coated on HPG/PEI electrodes exhibited an enhanced ET rate of 2.6-fold over only MB film, 4.3-fold over the MNP film alone, and nearly 2-fold over the MB/$MNP_{adsorbed}$ film (Scheme 1 and Figure 2). The observed enhanced ET rate indicates the crucial role of iron-oxide centers (Fe_3O_4) in MNP to act as efficient ET mediators for MB molecules, possibly via an electron-hopping mechanism.

The initial electron from the electrode can either reach the MB-heme center or an MNP-iron center in MB-MNP films. However, the observed direct electrochemical properties of MB-$MNP_{covalent}$ and MB/$MNP_{adsorbed}$ films correspond to MB and not to MNP (Figure 1). Hence, the initial electron transfer from the HPG/PEI electrode should be to the MB-heme center, which can subsequently undergo a hopping mechanism with closely arranged MB-heme centers and via MNP to distant MB-heme centers in the film (as proposed in Scheme 2). On the other hand, even if the initial electron from the electrode reaches an MNP-iron center in MB-$MNP_{covalent}$ film, it is possible that a subsequent hopping mechanism and significantly faster ET rate of MB over MNP (Figure 2) seems to have kinetically dominated to provide the observed MB electrochemistry in MB-MNP films.

Lisdat et al. demonstrated the occurrence of electron-hopping between protein redox centers in a multilayer film consist of up to 15 protein layers assembled alternatively with an anionic polyelectrolyte.[41] Hu et al. demonstrated an efficient electron-hopping mechanism mediated by gold nanoparticles to surface MB-heme centers over distances of >100 nm in films on basal plane graphite electrodes.[42]

Recently, a carbon ionic liquid electrode coated with carbon coated Fe_3O_4 nanospindles, MB, chitosan, and another coupling ionic liquid constructed in a stepwise manner to form a stable film was used to study the direct electrochemistry of cast MB.[43] The authors suggested the role of Fe_3O_4 nanospindles to act as an electron transfer mediator between the MB heme center and the modified electrode surface. However, the redox property of Fe_3O_4 nanospindles alone in the absence of MB was not detailed.[43]

The observed highly enhanced ET rate of MB-$MNP_{covalent}$ film over MB/$MNP_{adsorbed}$ film (Figure 2) in our work further suggests the existence of additional favorable factors to offer a better ET property in covalent MB-MNP films. The covalent immobilization of MB to MNP provides amide bond centers in MB-$MNP_{covalent}$ films that are absent in the case of physisorbed

Scheme 2. Long-Range Electron-Hopping Mechanism Occurring in MB-$MNP_{covalent}$ Films That Is Effectively Mediated by MNP and Further Facilitated by Intramolecular H-Bond Network between Amide Bonds (Connecting MB and MNP Covalently)[a]

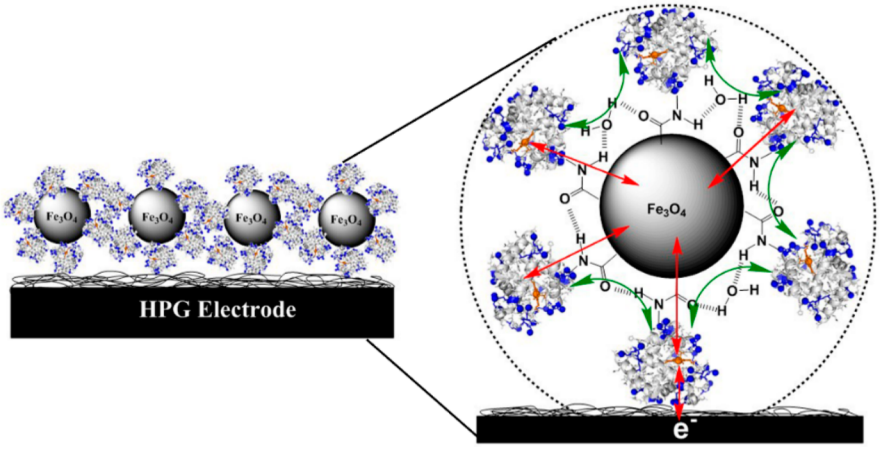

[a]The additional role of water molecules in enhancing the long-range electron hopping, via intermolecular H-bonding between water molecules and with the amide bond centers, is also illustrated.

$MB/MNP_{adsorbed}$ film. The property of amide bond centers in mediating an electron-hopping mechanism between an electrode and helical ferrocene oligopeptide, aided by an intramolecular H-bond network, has been recently proposed.[44] A similar hopping phenomenon is projected to occur in the designed $MB\text{-}MNP_{covalent}$ films to provide the observed largest ET rate (Figure 2). Additionally, the contribution of a H-bonded network formed by internal amide bonds in self-assembled monolayers on gold in attaining long-range electron transfer processes was suggested.[45]

Very recently, the effectiveness of short-range H-bonds to efficiently transport ET processes between single molecules was demonstrated.[46] Additionally, it has been shown that water channels that follow the Brownian dynamics can mediate both short- and long-range electron self-exchange processes between redox protein molecules.[47]

On the basis of the obtained results in this work and in reference to the findings from prior studies,[43−47] we propose an electron-hopping mechanism occurring in $MB\text{-}MNP_{covalent}$ films that involve long-range electron-hopping mediated by MNP to MB molecules and additionally facilitated by a H-bond network formed between amide bonds (i.e., −COOH of MNP with $-NH_2$ groups of MB forming an amide bond as a result of covalent attachment, as detailed above) both directly and via water molecules present in the electrolyte buffer (Scheme 2).

Interestingly, the ET rate of $MB/MNP_{adsorbed}$ film appears nearly to be the additive rates of MNP and MB films alone. This suggests the existence of similar hopping phenomenon occurring in these electrostatically assembled noncovalent films, and further indicates the absence of additional hopping forces such as from the amide bonds, as proposed to be present in $MB\text{-}MNP_{covalent}$ films (Scheme 2).

The rate of electron-transfer reported between the electrode and MB in certain magnetic nanoparticles-based studies were small and in the range of 3.0−3.6 s^{-1}.[18−21] This could arise from the buried inner Fe_3O_4 structure of MNP with an insulating outer oxide layer as used in several prior reports for MB immobilization. In addition, dry-coated films of MB on MNP-modified electrodes may have poor control over the arrangement and stability of protein molecules in films.

Catalytic Peroxide-Reduction Efficiency. The following order of catalytic peroxide reduction current density was exhibited by the designed MB films (Figure 5): $MB\text{-}MNP_{covalent}$ > $MB/MNP_{adsorbed}$ > only MNP > only MB. The enhancements in the reduction current density were in good agreement with the ET rates of $MB\text{-}MNP_{covalent}$ and $MB/MNP_{adsorbed}$ films. On the other hand, although the direct ET rate of only MB film was slightly greater than the MNP film alone, the observed order of catalytic current density was opposite. This is due to the greater proportion of electroactive concentration of MNP present in HPG/PEI film than in MB molecules (Figure 1) under the experimental conditions followed. This observation further indicates the presence of an effective electron hopping mechanism occurring between iron centers of large MNP (100 nm hydrodynamic diameter, Chemicell Inc.) in MNP films.

The apparent Michaelis−Menten constant (eq 2), K_M, was found to be 1.36 (±0.2) mM for $MB\text{-}MNP_{covalent}$, 1.15 (±0.05) mM for $MB/MNP_{adsorbed}$, 1.6 (±0.2) mM for only MB, and 2.9 (±0.1) mM for only MNP film (Figure 5, N = 3 repeats). The smaller K_M values of $MB\text{-}MNP_{covalent}$ and $MB/MNP_{adsorbed}$ films over either MB or MNP film alone suggest the advantages of incorporating MNP into the natural elegantly designed redox enzymes to achieve catalysis with exceedingly strong affinity for substrates and highly enhanced current density (Figure 5). The obtained apparent K_M of $MB\text{-}MNP_{covalent}$ films is similar to that reported for MB films on carbon-coated Fe_3O_4-nanospindles modified carbon ionic-liquid electrodes toward reducing trichloroacetic acid.[43]

The observed order of relative catalytic reduction efficiency (10^4 k_{cat}/K_M in M^{-1} s^{-1}) for the designed films was in the following order (Figure 5 and eq 2): $MB\text{-}MNP_{covalent}$ (14.2 ± 0.7) ≈ $MB/MNP_{adsorbed}$ (14.8 ± 1.0) > only MB (5.5 ± 0.4) > only MNP (5.2 ± 0.5). The obtained value of k_{cat}/K_M of only MB films is in good agreement with that reported for MB films assembled with polyions on pyrolytic graphite electrodes[32] and thus validates the accuracy of measurements performed in this study. More interestingly, the catalytic efficiency of MNP-MB films is improved by at least 2.5-times in comparison to only the MB film or the MNP film alone. Despite the fact that comparable catalytic efficiency was observed between the covalent and physisorbed MB films on MNPs, the $MB\text{-}MNP_{covalent}$ film displayed significantly higher peroxide reduction current density over $MB/MNP_{adsorbed}$ film, a property that is preferred in the design of bioreactors for chemical synthesis and other enzymatic electrochemical devices.

In addition, we found that $MB\text{-}MNP_{covalent}$ suspension in PBS was more stable than the $MB/MNP_{adsorbed}$ suspension in PBS. After 1 week of storage in PBS at 4 °C, the constructed film of $MB\text{-}MNP_{covalent}$ on HPG/PEI electrodes retained ∼85% of the initial oxygen reduction limiting-current, while the retention in limiting-current for $MB/MNP_{adsorbed}$ film was only ∼60%. Taken together, we have demonstrated that the rate of electron transfer and catalytic efficiency of either MB or MNP alone can be significantly amplified upon the conjugation of both together (Figures 2−5). In addition, the covalent strategy offered better electrochemical, catalytic, and stability properties than the corresponding physisorbed films. This suggests the usefulness of designing metalloenzyme-$MNP_{covalent}$ films to achieve efficient direct ET and in the development of efficient bioreactors for fine chemical synthesis.

■ CONCLUDING REMARKS

The results presented above provide the first mechanistic insights into the fundamental electrochemical and catalytic properties of a heme redox protein when combined with magnetic nanoparticles. The results obtained suggest that one can favorably tune the rates of ET and electrocatalysis of a metalloenzyme film on an electrode by simple chemical conjugation with functionalized magnetic nanoparticles, requiring only minimal enzyme amount. The large surface area of MNP with appropriate functional groups can enable the high density attachment of protein molecules in stable form along with a superior electronic connectivity to the electrode suitable for constructing novel bioreactors for chemical synthesis. We suggest the existence of an efficient long-range electron-hopping mechanism as the major driving force for the observed amplified ET and catalytic rates of MNP-protein films on electrodes. The findings of this study thus possess considerable potential in the development of novel efficient biosensors, nanochip-devices, bioreactors, and fundamental mechanistic studies of other enzyme films (including redox enzymes with buried redox centers) by connecting them efficiently to electrode surfaces via MNP.

AUTHOR INFORMATION

Corresponding Author

*E-mail: gopan.krishnan@okstate.edu.

Notes

The authors declare no competing financial interest.

ACKNOWLEDGMENTS

The financial support by the Oklahoma State University is greatly acknowledged. The authors thank Dr. K. S. Prasad for helpful discussions.

REFERENCES

(1) Krishnan, S.; Rusling, J. F. Thin Iron Heme Enzyme Films on Electrodes and Nanoparticles for Biocatalysis. In *New and Future Developments in Catalysis*; Suib, S. L., Ed.; Elsevier Publishers: Amsterdam, The Netherlands, 2013; pp 125−147.

(2) Armstrong, F. A.; Belsey, N. A.; Cracknell, J. A.; Goldet, G.; Parkin, A.; Reisner, E.; Vincent, K. A.; Wait, A. F. *Chem. Soc. Rev.* **2009**, *38*, 36−51.

(3) Armstrong, F. A.; Hirst, J. *Proc. Natl. Acad. Sci. U.S.A.* **2011**, *108*, 14049−14054.

(4) Hsing, I.-M.; Xu, Y.; Zhao, W. *Electroanalysis* **2007**, *19*, 755−768.

(5) Hill, H. D.; Mirkin, C. A. *Nat. Protoc.* **2006**, *1*, 324−336.

(6) Wang, S. X.; Li, G. *IEEE Trans. Magn.* **2008**, *44*, 1687−1702.

(7) Zhang, Y.; Zhou, D. *Expert Rev. Mol. Diagn.* **2012**, *12*, 565−571.

(8) Mani, V.; Chikkaveeraiah, B. V.; Rusling, J. F. *Expert Rev. Mol. Diagn.* **2011**, *5*, 381−391.

(9) Haun, J. B.; Yoon, T.-J.; Lee, H.; Ralph, W. *Nanomed. Nanobiotechnol.* **2010**, *2*, 291−304.

(10) Rusling, J. F.; Sotzing, G.; Papadimitrakopoulos, F. *Bioelectrochemistry* **2009**, *76*, 189−194.

(11) Wang, W.; Xu, Y.; Wang, D. I. C.; Li, Z. *J. Am. Chem. Soc.* **2009**, *131*, 12892−12893.

(12) Gao, L.; Zhuang, J.; Nie, L.; Zhang, J.; Zhang, Y.; Gu, N.; Wang, T.; Feng, J.; Yang, D.; Perrett, S.; Yan, X. *Nat. Nanotechnol.* **2007**, *2*, 577−583.

(13) Zhuang, J.; Fan, K.; Gao, L.; Lu, D.; Feng, J.; Yang, D.; Gu, N.; Zhang, Y.; Liang, M.; Yan, X. *Mol. Pharm.* **2012**, *9*, 1983−1989.

(14) Wiogo, H. T. R.; Lim, M.; Bulmus, V.; Gutierrez, L.; Woodward, R. C.; Amal, R. *Langmuir* **2012**, *28*, 4346−4356.

(15) Wang, J.; Wang, X.; Ren, L.; Wang, Q.; Li, L.; Liu, W.; Wan, Z.; Yang, L.; Sun, P.; Ren, L.; Li, M.; Wu, H.; Wang, J.; Zhang, L. *Anal. Chem.* **2009**, *81*, 6210−6217.

(16) Hayes, M. A.; Petkus, M. M.; Garcia, A. A.; Taylor, T.; Mahanti, P. *Analyst* **2009**, *134*, 533−541.

(17) Sharma, R.; Haik, Y.; Chen, C. J. *J. Exp. Nanosci.* **2007**, *2*, 127−138.

(18) Qiua, J.-D.; Peng, H.-P.; Liang, R.-P.; Xi, X.-H. *Biosens. Bioelectron.* **2010**, *25*, 1447−1453.

(19) Peng, H.-P.; Liang, R.-P.; Qiu, J.-D. *Biosens. Bioelectron.* **2011**, *26*, 3005−3011.

(20) Peng, H.-P.; Liang, R.-P.; Zhang, L.; Qiu, J.-D. *Electrochim. Acta* **2011**, *56*, 4231−4236.

(21) Peng, H.-P.; Liang, R.-P.; Zhang, L.; Qiu, J.-D. *J. Electroanal. Chem.* **2013**, *700*, 70−76.

(22) Xu, Q.; Bian, X.-J.; Li, L.-L.; Hu, X.-Y.; Sun, M.; Chen, D.; Wang, Y. *Electrochem. Commun.* **2008**, *10*, 995−999.

(23) Sander, R. *Henry's Law Constants (Solubilities)*, version 3; Compilation of Henry's law constants for inorganic and organic species of potential importance in environmental chemistry, 1999. Available at www.henrys-law.org.

(24) Cracknell, J. A.; Wait, A. F.; Lenz, O.; Friedrich, B.; Armstrong, F. A. *Proc. Natl. Acad. Sci. U.S.A.* **2009**, *106*, 20681−20686.

(25) Copeland, D. M.; Soares, A. S.; West, A. H.; Richter-Addo, G. B. *J. Inorg. Biochem.* **2006**, *100*, 1413−1425.

(26) Goto, Y.; Fink, A. L. *J. Mol. Biol.* **1990**, *214*, 803−805.

(27) Righetti, P. G.; Drysdale, J. W. *Isoelectric Focusing Laboratory Techniques in Biochemistry and Molecular Biology*; Work, T. S., Work, E., Eds.; North Holland Publishing Co.: Amsterdam, The Netherlands, 1976.

(28) Leaist, D. G. *J. Solution Chem.* **1989**, *18*, 421−435.

(29) Kostka, J. E.; Nealson, K. H. *Environ. Sci. Technol.* **1995**, *29*, 2535−2540.

(30) Bard, A.; Faulkner, L. R. In *Electrochemical Methods: Fundamentals and Applications*, 2nd ed.; Wiley: New York, 2001.

(31) Li, N.; Xu, J.-Z.; Yao, H.; Zhu, J.-J.; Chen, H.-J. *J. Phys. Chem. B* **2006**, *110*, 11561−11565.

(32) Krishnan, S.; Abeykoon, A.; Schenkman, J. B.; Rusling, J. F. *J. Am. Chem. Soc.* **2009**, *131*, 16215−16224.

(33) Krishnan, S.; Wasalathanthri, D.; Zhao, L.; Schenkman, J. B.; Rusling, J. F. *J. Am. Chem. Soc.* **2011**, *133*, 1459−1463.

(34) Krishnan, S.; Rusling, J. F. *Electrochem. Commun.* **2007**, *9*, 2359−2363.

(35) Hirst, J.; Armstrong, F. A. *Anal. Chem.* **1998**, *70*, 5062−5071.

(36) Laviron, E. *J. Electroanal. Chem.* **1979**, *101*, 19−28.

(37) Guto, P. M.; Rusling, J. F. *J. Phys. Chem. B* **2005**, *109*, 24457−24464.

(38) Munge, B.; Estavillo, C.; Schenkman, J. B.; Rusling, J. F. *ChemBioChem* **2003**, *4*, 82−89.

(39) Heering, H. A.; Hirst, J.; Armstrong, F. A. *J. Phys. Chem. B* **1998**, *102*, 6889−6902.

(40) Krishnan, S.; Schenkman, J. B.; Rusling, J. F. *J. Phys. Chem. B* **2011**, *115*, 8371−8380.

(41) Beissenhirtz, M. K.; Scheller, F. W.; Stocklein, W. F. M.; Kurth, D. G.; Mohwald, H.; Lisdat, F. *Angew. Chem., Int. Ed.* **2004**, *43*, 4357−4360.

(42) Chai, H.; Liu, H.; Guo, X.; Zheng, D.; Kutes, Y.; Huey, B. D.; Rusling, J. F.; Hu, N. *Electroanalysis* **2012**, *24*, 1129−1140.

(43) Ke, Y.; Zeng, Y.; Pu, X.; Wu, X.; Li, L.; Zhu, Z.; Yu, Y. *RSC Adv.* **2012**, *2*, 5676−5682.

(44) Yu, J.; Zvarec, O.; Huang, D. M.; Bissett, M. A.; Scanlon, D. B.; Shapter, J. G.; Abell, A. D. *Chem. Commun.* **2012**, *48*, 1132−1134.

(45) Sek, S.; Bilewicz, R. *J. Electroanal. Chem.* **2001**, *509*, 11−18.

(46) Nishino, T.; Hayashi, N.; Bui, P. T. *J. Am. Chem. Soc.* **2013**, *135*, 4592−4595.

(47) Lin, J.; Balabin, I. A.; Beratan, D. N. *Science* **2005**, *310*, 1311−1313.